



Contents lists available at ScienceDirect

Radiation Measurements

journal homepage: www.elsevier.com/locate/radmeas

Characterization of $\text{YVO}_4:\text{Eu}^{3+}$ scintillator as detector for Fiber Optic Dosimetry

N. Martínez ^{a,*}, A. Rucci ^b, J. Marcazzó ^a, P. Molina ^a, M. Santiago ^a, W. Cravero ^b

^a Instituto de Física Arroyo Seco (UNCPBA) and CIFICEN (UNCPBA-CICPBA-CONICET), Pinto 399, 7000 Tandil, Argentina

^b Instituto de Física del Sur (IFISUR), Departamento de Física, UNS-CONICET, Argentina

HIGHLIGHTS

- $\text{YVO}_4:\text{Eu}$ -based dosimetric probes are suitable for real time dosimetry.
- $\text{YVO}_4:\text{Eu}$ response shows repeatability and independence with accumulated dose within therapeutic range.
- Isotropic response is observed if the detector is spherically shaped.

ARTICLE INFO

Article history:

Received 1 October 2016
 Received in revised form
 2 February 2017
 Accepted 14 March 2017
 Available online xxx

Keywords:

Insert

ABSTRACT

Fiberoptic dosimetry (FOD) is an experimental technique suitable for in-vivo, real time dosimetry in radiotherapy treatments. In a previous work it was found that $\text{YVO}_4:\text{Eu}$ is a scintillator suitable to be employed as scintillator for FOD in pulsed MV photon beams. $\text{YVO}_4:\text{Eu}$ -based FOD probes have shown several positive characteristics: temperature independence; no previous irradiation needed; good spatial resolution. In this paper others dosimetric characteristics have been investigated for the first time. Suitability for real time dosimetry has been determined by simultaneous measurement with a ionization chamber; off axis profile have been obtained in order to assess spatial resolution of the FOD system when used in fields having a size of $3 \times 3\text{cm}^2$ and $1 \times 1\text{cm}^2$; angular dependence has been studied for probes with cylindrical and quasi-spherical geometry showing the influence of the detector shape on its isotropy. Additionally, PDD curves resulting from Monte Carlo simulations have been successfully compared to experimental curves.

© 2017 Elsevier Ltd. All rights reserved.

1. Introduction

The development of radiotherapy techniques such as intensity-modulated radiotherapy, volumetric modulated arc therapy or stereotactic radiosurgery, has lead to highly conformed treatments, which maximize dose on target and minimize dose in adjacent organs at risk. Planning potentially involves hypofractionated treatments with large doses per fraction. This fact demands innovative approaches to patient safety including in-vivo dose verification, as international organizations involved recommended (Yorke et al., 2005; IAEA, 2014), which prompt in turn to the

development and research of new techniques for in-vivo dosimetry. Several methods have been developed in the last years, each one with comparative advantages and disadvantages for different measurements conditions (Mijnheer et al., 2013).

In this context, a technique known as Fiber Optic Dosimetry (FOD) has become an attractive alternative to traditional dosimetry systems due to the small size of the radiation detectors employed (Beddar et al., 1992a,b; Létourneau et al., 1999; Huston et al., 2001; Polf et al., 2004; Andersen et al., 2009; Santos et al., 2015). This technique has high spatial resolution and is capable of estimating the dose rate in real time. FOD relies on using a small piece of scintillator ($\sim 1\text{mm}^3$) attached to the end of an optical fiber, which guides the light emitted by the scintillator during irradiation outside the treatment room up to a light detector. In general, the intensity of the scintillating light or radioluminescence (RL) can be regarded as proportional to the dose rate absorbed by the scintillator (Beaulieu et al., 2013).

* Corresponding author.

E-mail addresses: nahuelm@exa.unicen.edu.ar (N. Martínez), alexisrucci@gmail.com (A. Rucci), jmarcass@exa.unicen.edu.ar (J. Marcazzó), pmolina@exa.unicen.edu.ar (P. Molina), msantiag@exa.unicen.edu.ar (M. Santiago), wcravero@uns.edu.ar (W. Cravero).

The main drawback of this technique is the presence of the light produced in the optical fiber itself during irradiation, dubbed stem effect, which adds to the radioluminescence signal and produces a bias of the estimated dose rate. The stem effect has two components, namely, the in-fiber Cerenkov radiation and intrinsic luminescence of the optical fiber (Beddar et al., 1992a,b). The stem effect for fast organic plastic scintillators can be reduced by at least three methods as reported by Liu et al. (2011). For slow materials, a temporal discrimination method can be used when the irradiation source is pulsed, for instance, in medical linear accelerator beams commonly used for radiotherapy (Clift et al., 2002). This method is effective when the radioluminescence signal has a lifetime which is long compared with the duration of the radiation pulses (Martínez et al., 2015; Buranurak and Andersen, 2016).

Standard Imaging provided the medical community with the Exradin W1. This was the first commercially available FOD system for dosimetry in external-beam radiotherapy. This detector was characterized for the first time by Beierholm et al. (2015), giving place to a number of debates related to the energy dependence of the Cerenkov light ratio (CLR) coefficient (Carrasco et al., 2015a,b; Beierholm et al., 2015). Far away from a closed debate, the research for new scintillators is currently of interest in order to FOD become a mature dosimetric technique (Mattia et al., 2015; Ramírez et al., 2016; Teichmann et al., 2016; Rahman et al., 2016).

Recently, preliminary results about the performance of YVO₄:Eu-based FOD probes has been reported (Martínez et al., 2015). Although YVO₄:Eu has an effective atomic number higher than soft tissue, YVO₄:Eu-based probes demonstrated to be suitable for real-time dosimetry in those cases when the irradiation field size is smaller than $3 \times 3 \text{ cm}^2$. The temperature dependence of the detector response was found to be lower than those of plastic scintillators and its spatial resolution was higher than that of a PinPoint ion chamber.

In this work additional characterization of the YVO:Eu-based FOD probe has been carried out. In particular, repeatability of detector response and suitability for real time dose assessment have been investigated. Besides, the capability of the FOD system to characterize the shape of small size fields and angular dependence of the signal have been studied. Additionally, MC simulations have carried out in order to increase certainty to established hypotheses about discrepancies in PDD measurements.

2. Materials and methods

2.1. Scintillator dosimetry system

Measurements were made using a dosimetric probe based on YVO₄:Eu fabricated identically to the one described in Martínez et al. (2015). In this case, YVO₄:Eu powder (Phosphor Technologies, UK) was pressed inside a 1 mm inner diameter, 3 mm length PVC cylindrical container, which was coupled the optical fiber end. Only for angular dependence measurements another probe was employed. In this case YVO₄:Eu powder was dispersed inside a glue droplet (NOA 68, Norland Adhesives, USA) and coupled to the fiber-end. Fig. 1 shows the probe before coating its end with water-lightproof paint. It is apparent that in this case the scintillator features a quasi-spherical shape.

The scintillation light emerging from the optical fiber was measured using a Hamamatsu H9319-02 phototube in photon counting mode. Counts per second were integrated using a National Instruments USB-6251 DAQ. Maximum temporal resolution achievable was 10 μs .

In-situ measurements were made in a Varian de 6 MV LINAC (1 MU = 1.065 cGy in reference conditions). A scheme of the in-situ experimental setup is shown in Fig. 2.

2.2. Temporal discrimination of stem effect

To eliminate the stem effect, the temporal method was used in all measurements. LABVIEW software was used to control the NI USB-6251 by integrating only counts detected in a 1880 μs long window starting 20 μs after each LINAC pulse reaching the detector. The lapse between consecutive LINAC pulses was 4.5 ms long. Since YVO₄:Eu decay time is 0.5 ms, no correction for signal superposition is needed. Using this method the stem effect is eliminated completely.

2.3. Real time response and repeatability

In order to determine whether the RL signal of the FOD probe is proportional to the dose rate as measured by a standard ion chamber, both detectors were simultaneously delivered a dose of 600 MU (6.39 Gy) in a water phantom and their signals were compared. The sensitive end of the FOD probe was placed 4 cm apart from the center of a $12 \times 12 \text{ cm}^2$ field (100 cm source to surface distance-SSD, 5 cm water depth). A PTW 31014 PinPoint ion chamber (0.015 cm^3) was placed in the symmetrically opposite point with respect to the beam axis and its signal was measured simultaneously. The ion chamber yield was acquired by means of a UNIDOS E PTW electrometer.

The stability of RL response was determined by repeating measurements in identical conditions. The FOD probe was 10 times consecutively delivered a dose of 100 MU (1.065 Gy) in reference conditions (SSD = 100 cm; $10 \times 10 \text{ cm}^2$ field size, 1.4 cm water depth) with 1 min interval between irradiations. The average counting rate and the area under the curve RL versus time (integrated counts) were determined.

2.4. Off axis profiles

The spatial resolution of the FOD system was evaluated by measuring off-axis profiles corresponding to $3 \times 3 \text{ cm}^2$ and $1 \times 1 \text{ cm}^2$ field sizes. A water phantom with dimensions 400(L) \times 400(W) \times 400(D)mm featuring an ad-hoc motorized scan system was employed. For the sake of comparison off-axis profiles were also determined by means of the PinPoint PTW ion chamber (please see above). The sensitive end of the detectors were moved along the irradiation field at 0.15 cm/s within a plane orthogonal to the beam. Ion chamber readings were performed every 1s while the FOD probe signal was acquired every 0.05s. The measurements were made at SSD = 100 cm and at 1.4 cm water depth. PinPoint axis was oriented parallel to the beam and FOD axis was oriented perpendicularly to the beam.

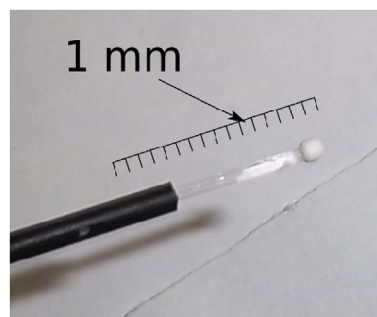


Fig. 1. Detail of quasi-spherical YVO₄:Eu-based detector coupled to the end of the optical fiber.

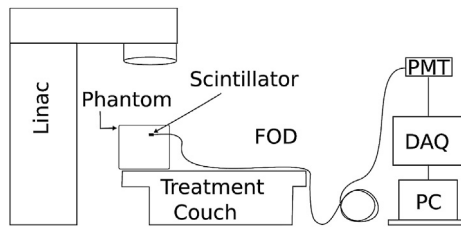


Fig. 2. Experimental setup corresponding to In-situ measurements.

2.5. Angular dependence

In order to evaluate the angular response of the $\text{YVO}_4:\text{Eu}$ -based detector the end of the FOD probe was placed at the center of a spherical lab-made phantom (20 cm diameter) made of gelified Agar (Aranda-Lara et al., 2014) and irradiated employing a $5 \times 5 \text{ cm}^2$ field size at different gantry positions. The scintillator was located exactly at the center of the phantom, which, in turn, coincided with the LINAC isocenter. As can be seen in Fig. 3 two configurations were employed. In one of them different azimuthal angles were spanned, say, the fiber was placed vertically and parallel to the plane spanned by the beam. Angle steps of 45° were employed starting from 90° up to 270° .

In the other configuration, the fiber axis was placed horizontally and orthogonal to the plane spanned by the gantry. In this case angle steps of 45° were employed starting from 90° up to 270° , too.

2.6. Monte Carlo simulations

It was previously reported that in percentage depth dose (PDD) experiments the $\text{YVO}_4:\text{Eu}$ FOD probe overestimates the dose with respect to an ion chamber if the field size is larger than $3 \times 3 \text{ cm}^2$ (Martínez et al., 2015). Martínez et al. interpreted this observation as a result of the higher effective atomic number of $\text{YVO}_4:\text{Eu}$ ($Z_{\text{eff}} = 25.4$) with respect to that of water ($Z_{\text{eff}} = 7.4$). For this reason, as the dimensions of the field decreases, the difference between the signal of the probe and the signal of the ion chamber also decreases. Although this statement is plausible, it should be confirmed by means of Monte Carlo simulations in order to discard other causes, which could be related to the scintillation process instead of to the energy absorption process.

PDD curves of the $\text{YVO}_4:\text{Eu}$ FOD probe were simulated by Monte Carlo simulations and compared to PPD curves obtained experimentally. For Monte Carlo simulations, a hybrid virtual source model based on IAEA phase space data base was used [Rucci et al., 2014; Capote et al., 2006]. With this method it is possible to reproduce dose data for any field size and from different clinical accelerators with uncertainties below $3\%/2 \text{ mm}$ [Rucci et al., 2016]. The $\text{YVO}_4:\text{Eu}$ detector was simulated with an 8 mm^3 cube. This

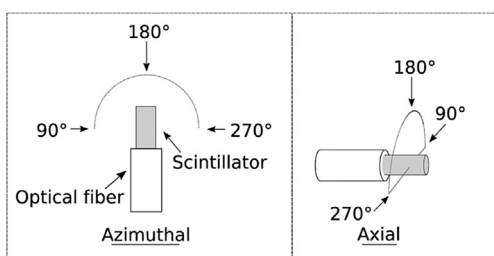


Fig. 3. Scheme of the experimental setup employed for the angular dependence measurements. In the first case the azimuth was changed (FOD axis vertically oriented). In the second case the axial angle was varied (FOD axis horizontally oriented).

volume ensures that statistical fluctuations are well below statistical uncertainties from the virtual source model. All calculations were performed using PENELOPE Monte Carlo code [Salvat et al., 2006]. We used cut off energies of 100 keV for electrons and 10 keV for photons. For the sake of comparison, the absorbed dose by a similar volume of water in identical conditions was also estimated by MC calculations.

3. Results and discussion

3.1. Real time response and repeatability

In Fig. 4 the result of the simultaneous measurement of the FOD and ion chamber signals in a $12 \times 12 \text{ cm}^2$ field size is shown. Both signals match during almost all exposure time and differ only by discrepancies well within the resolution of each detector. No systematic deviation was found in exposures up to 600 MU (6 Gy), showing that at doses characteristic of radiotherapy treatments the FOD detector response is similar to that of the ion chamber. This measurement was repeated 10 times, delivering 60 Gy in total to FOD detector without noting any decrease on response.

In Fig. 5 the repeatability of the RL signal of the $\text{YVO}_4:\text{Eu}$ based FOD detector is shown. Circles correspond to the averaged counts per second, while the integrated counts are depicted as hollow squares. It can be seen from the figure that the latter readings vary less than 0.5%. This difference matches with the expected fluctuations for the LINAC employed, as measured during routine calibration with a ionization chamber. In the same sense, variation in dose rate (in the order of 2,5%) are also attributable to LINAC behaviour that shows an increases of average dose rate in consecutive exposures. The lower value of the four initial dose rate readings can be easily ascribed to a warm-up effect corresponding to the LINAC. Although the dose rate stabilizes at the fifth measurement, the integrated counts were constant from the first irradiation, what implies that the total dose delivered by de LINAC in each irradiation was constant along the ten measurements.

3.2. Off axis profile

Off axis profile measurements in a $3 \times 3 \text{ cm}^2$ and $1 \times 1 \text{ cm}^2$ field sizes are shown in Figs. 6 and 7 respectively.

Differences between $\text{YVO}_4:\text{Eu}$ and PTW PinPoint signal as shown in the upper plot show that in penumbra region discrepancies reach 5%. As is expected (Laub and Wong, 2003), volumetric effect in the PinPoint ion chamber (15 mm^3) response can lead to an overestimation in the bottom of penumbra and a sub-estimation in the upper region. Results demonstrate that $\text{YVO}_4:\text{Eu}$ based probe ($\sim 0.5 \text{ mm}^3$) has a higher spatial resolution than PinPoint Ion chamber.

In $1 \times 1 \text{ cm}^2$ field the differences are slightly smaller than in the previous case. This result, however, is probably due to the fact that the penumbra region is actually wider as a result of the smallness of the field. In future works $\text{YVO}_4:\text{Eu}$ based probe should be compared to dosimeters with higher spatial resolution, such as diamond detectors or unshielded diodes.

3.3. Angular dependence

Both $\text{YVO}_4:\text{Eu}$ based probes (cylindrical and quasi-spherical detectors) show independence of their RL emission for different axial angles, as expected given the cylindrical symmetry of the experimental setup. Nevertheless, in azimuthal angle experiments the cylindrical probe shows a strong dependence due to changes in effective active area irradiated at different angles. In Fig. 8 the results for angular dependence in azimuthal angle in both probes is

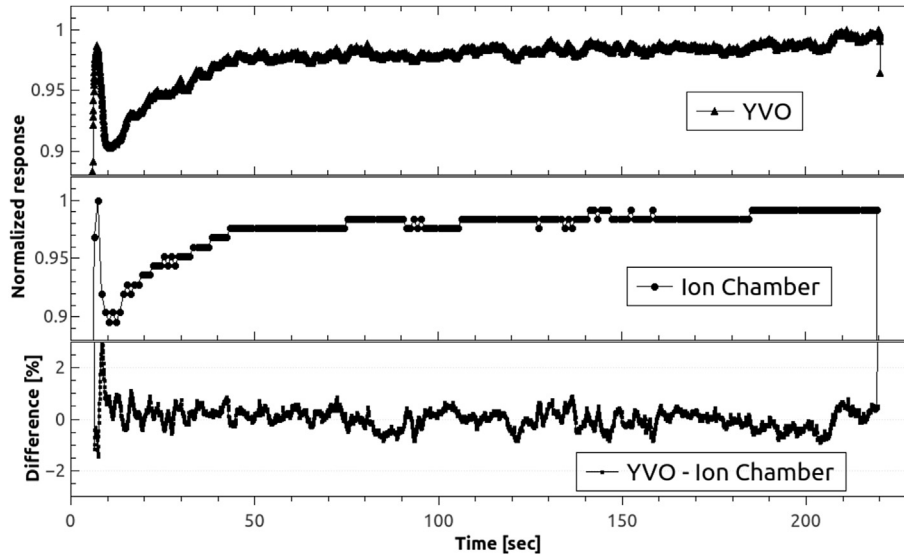


Fig. 4. Response of YVO₄:Eu detector and a PTW PinPoint ion chamber irradiated at 600 MU.

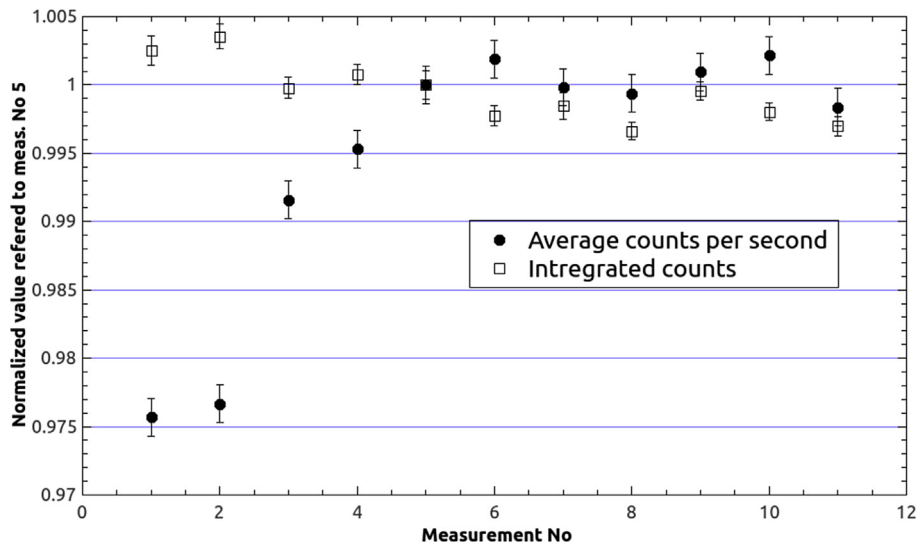


Fig. 5. Repeatability of RL signal with YVO₄:Eu based FOD detector.

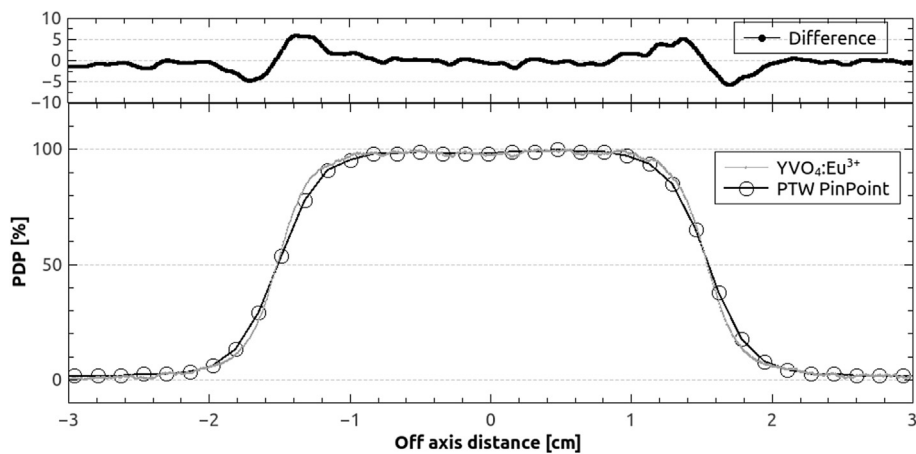


Fig. 6. Off axis percentage dose profile. Field size 3 × 3 cm².

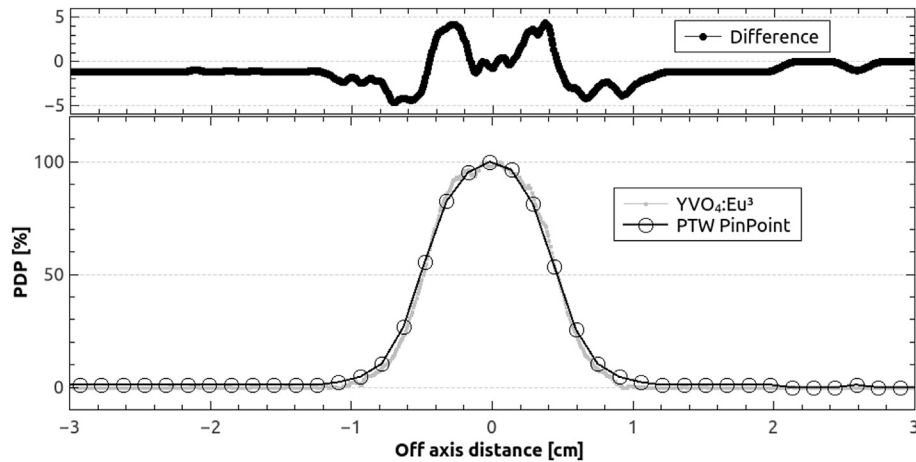


Fig. 7. Off axis percentage dose profile. Field size $1 \times 1 \text{ cm}^2$.

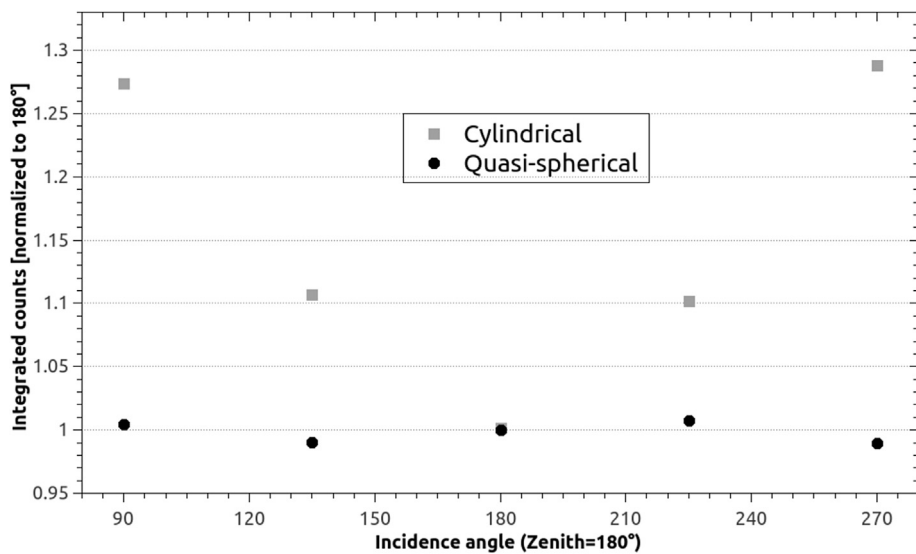


Fig. 8. Comparison between angular dependence in cylindrical and quasi-spherical probes.

shown.

It can be seen from figure that cylindrical probe reaches differences close to 30% when azimuthal angle is changed 90° . This result is in accordance to obtained with others detectors (Lambert et al., 2006; Hyer et al., 2009; Qin et al., 2013) and can be explained by the high efficiency of the scintillator and the effective area of active volume confronted to primary beam. On the other hand, the quasi-spherical probe shows RL response independent to the incident angle with observed variation that are less than 2%, a value expected for this configuration. Construction of the quasi-spherical probe proved to be a feasible solution to lead with the problem of azimuthal angular dependence of the detector. In addition quasi-spherical probe present higher RL emission than cylindrical probe due to the possibility of increase powder deposition in fiber optic end.

3.4. Monte Carlo simulations

In Fig. 9 and Fig. 10 PDD curves obtained with the FOD probe and the ion chamber (field sizes of $2 \times 2 \text{ cm}^2$ and $10 \times 10 \text{ cm}^2$) are compared with Monte Carlo simulated PDD curves corresponding to an 8 mm^3 cube of $\text{YVO}_4:\text{Eu}$ and an identical volume of water

respectively.

The simulations reproduce with very good agreement the experimental results in both field sizes. This result confirms the hypothesis that the dose overestimation is due to the influence of the high Z_{eff} of the $\text{YVO}_4:\text{Eu}$ based probe, which increases the sensitivity of the detector to secondary radiation. Using MC simulations calibration factors could lead to an appropriate use of $\text{YVO}_4:\text{Eu}$ based probe in specific configurations.

4. Conclusions

The present work, in addition to previous research (Molina et al., 2012; Martínez et al., 2015), supports the development of FOD detectors based on $\text{YVO}_4:\text{Eu}^{3+}$ for small field real-time dosimetry. Response stability has been demonstrated with a repeatability better than 0.5%. Comparison with the response of a ion chamber demonstrates that the FOD probe performs well as real time dosimetry system. Off axis profile measurements shows that $\text{YVO}_4:\text{Eu}$ based probes have a better spatial resolution than PinPoint ion chamber in 3×3 and $1 \times 1 \text{ cm}^2$. However, more studies are needed in order to determine maximum resolution of this FOD detector. High efficiency of the scintillator results in a

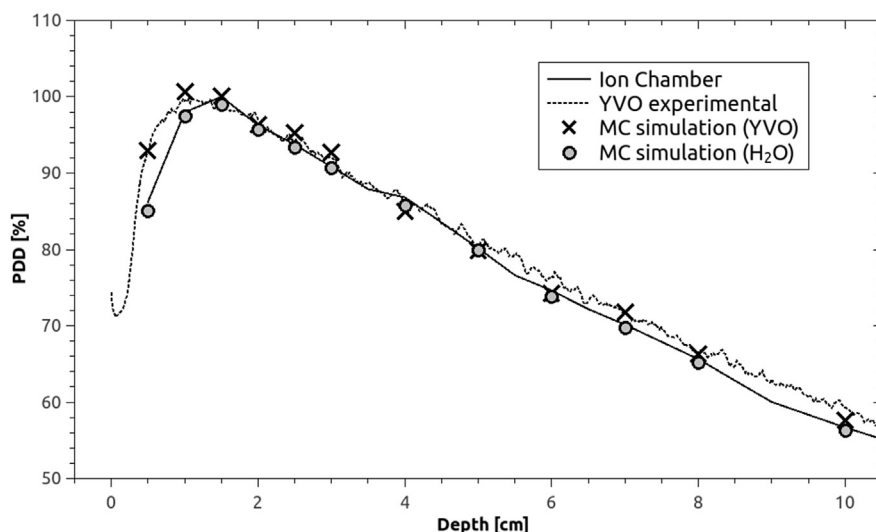


Fig. 9. Monte Carlo simulation for PDD in a 2×2 cm² field size.

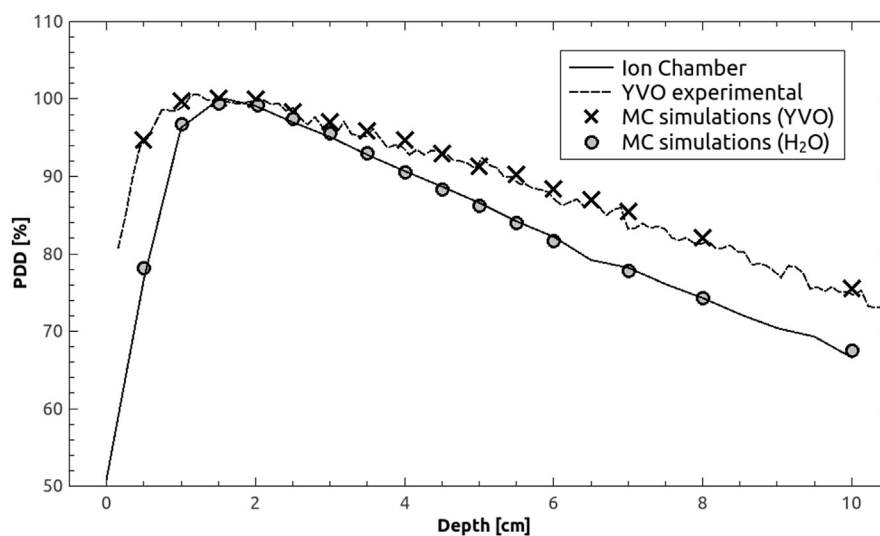


Fig. 10. Monte Carlo simulation for PDD in a 10×10 cm² field size.

strong angular dependence due to geometrical reasons. It was proved that the construction of a quasi-spherical probe provides a feasible solution to solve this problem. Monte Carlo simulated PDD curves agree very well with experimental results. This fact serves as an evidence that Monte Carlo corrections could be of help to compensate bias response of YVO₄:Eu due to its non-tissue-equivalence.

Acknowledgements

The authors acknowledge the financial support received from PICT 2015-1555 (ANPCyT, Argentina) and PIP 2015-2017 (CONICET, Argentina). They would also like to acknowledge to Dr. Héctor García for his assistance in gelified agar phantom construction.

References

- Andersen, Claus E., Kynde Nielsen, Soren, Christian Lindegaard, Jacob, Tanderup, Kari, 2009. Time-resolved in vivo luminescence dosimetry for online error detection in pulsed dose-rate brachytherapy. *Med. Phys. Med. Phys.* 36 (11), 5033. <http://dx.doi.org/10.1118/1.3238102>.
- Aranda-Lara, Liliana, Torres-García, Eugenio, Oros-Pantoja, Rigoberto, 2014. "Biological tissue modeling with agar gel phantom for radiation dosimetry of ^{99m}Tc. *Open J. Radiol. OJRad* 04 (01), 44–52. <http://dx.doi.org/10.4236/ojrad.2014.41006>.
- Beaulieu, L., Goulet, M., Archambault, L., Beddar, S., 06 2013. Current status of scintillation dosimetry for megavoltage beams. *J. Phys. Conf. Ser.* 444, 012013. <http://dx.doi.org/10.1088/1742-6596/444/1/012013>.
- Beddar, A.S., Mackie, T.R., Attix, F.H., 04 1992a. Cerenkov light generated in optical fibres and other light pipes irradiated by electron beams. *Phys. Med. Biol.* 37 (4), 925–935. <http://dx.doi.org/10.1088/0031-9155/37/4/007>.
- Beddar, A.S., Mackie, T.R., Attix, F.H., 10 1992b. Water-equivalent plastic scintillation detectors for high-energy beam dosimetry: I. Physical characteristics and theoretical considerations. *Phys. Med. Biol.* 37 (10), 1883–1900. <http://dx.doi.org/10.1088/0031-9155/37/10/006>.
- Beierholm, A.R., Behrens, C.F., Andersen, C.E., 07 2015. Comment on "characterization of the Exradin W1 scintillator for use in radiotherapy" [*med. Phys.* 42, 297–304 (2015)]. *Med. Phys. Med. Phys.* 42 (7), 4414–4416. <http://dx.doi.org/10.1118/1.4922656>.
- Buranurak, S., Andersen, C.e., 10 2016. Fiber-coupled Al₂O₃:C radioluminescence dosimetry for total body irradiations. *Radiat. Meas.* 93, 46–54. <http://dx.doi.org/10.1016/j.radmeas.2016.05.001>.
- Capote, R., Jeraj, R., Ma, C.M., Rogers, D.W.O., Sánchez-Doblado, F., Sempau, J., Seuntjens, J., Siebers, J.V., 2006. Phase-space database for external beam radiotherapy. In: *Summary Report of a Consultants' Meeting*. International

Atomic Energy Agency, Vienna.

- Carrasco, P., Jornet, N., Jordi, O., Lizondo, M., Latorre-Musoll, A., Eudaldo, T., Ruiz, A., Ribas, M., 07 2015b. Characterization of the Exradin W1 scintillator for use in radiotherapy. *Med. Phys. Med. Phys.* 42 (1), 297–304. <http://dx.doi.org/10.1118/1.4903757>.
- Carrasco, P., Jornet, N., Jordi, O., Lizondo, M., Latorre-Musoll, A., Eudaldo, T., Ruiz, A., Ribas, M., 07 2015b. Response to “comment on ‘characterization of the Exradin W1 scintillator for use in radiotherapy’” [med. Phys. 42, 297–304 (2015)]. *Med. Phys. Med. Phys.* 42 (7), 4417–4418. <http://dx.doi.org/10.1118/1.4922655>.
- Clift, M.A., Johnston, P.N., Webb, D.V., 04 2002. A temporal method of avoiding the Cerenkov radiation generated in organic scintillator dosimeters by pulsed mega-voltage electron and photon beams. *Phys. Med. Biol.* 47 (8), 1421–1433. <http://dx.doi.org/10.1088/0031-9155/47/8/313>.
- Huston, A.I., Justus, B.I., Falkenstein, P.I., Miller, R.W., Ning, H., Altemus, R., 09 2001. Remote optical fiber dosimetry. *Nucl. Instrum. Methods Phys. Res. Sect. B Beam Interact. Mater. Atoms* 184 (1–2), 55–67. [http://dx.doi.org/10.1016/s0168-583x\(01\)00713-3](http://dx.doi.org/10.1016/s0168-583x(01)00713-3).
- Hyer, Daniel E., Fisher, Ryan F., Hintenlang, David E., 2009. Characterization of a water-equivalent fiber-optic coupled dosimeter for use in diagnostic radiology. *Med. Phys. Med. Phys.* 36 (5), 1711. <http://dx.doi.org/10.1118/1.3116362>.
- IAEA, 2014. *Radiation Protection and Safety of Radiation Sources: International Basic Safety Standards*. International Atomic Energy Agency, Vienna, ISBN 978-92-0-135310-8.
- Lambert, J., Mckenzie, D.R., Law, S., Elsej, J., Suchowerska, N., 10 2006. A plastic scintillation dosimeter for high dose rate brachytherapy. *Phys. Med. Biol.* 51 (21), 5505–5516. <http://dx.doi.org/10.1088/0031-9155/51/21/008>.
- Laub, Wolfram U., Wong, Tony, 2003. The volume effect of detectors in the dosimetry of small fields used in IMRT. *Med. Phys. Med. Phys.* 30 (3), 341. <http://dx.doi.org/10.1118/1.1544678>.
- Létourneau, D., Pouliot, J., Roy, R., 1999. Miniature scintillating detector for small field radiation therapy. *Med. Phys. Med. Phys.* 26 (12), 2555. <http://dx.doi.org/10.1118/1.598793>.
- Liu, P.Z.Y., Suchowerska, N., Lambert, J., Abolfathi, P., Mckenzie, D.R., 08 2011. Plastic scintillation dosimetry: comparison of three solutions for the Cerenkov challenge. *Phys. Med. Biol.* 56 (18), 5805–5821. <http://dx.doi.org/10.1088/0031-9155/56/18/003>.
- Martinez, Nahuel, Teichmann, Tobias, Molina, Pablo, Sommer, Marian, Santiago, Martin, Henniger, Jürgen, Caselli, Eduardo, 12 2015. Scintillation properties of the YVO₄:Eu³⁺ compound in powder form: its application to dosimetry in radiation fields produced by pulsed mega-voltage photon beams. *Z. Für Med. Phys.* 25 (4), 368–374. <http://dx.doi.org/10.1016/j.zemedi.2015.04.001>.
- Mattia, Cristina De, Veronese, Ivan, Fasoli, Mauro, Chiodini, Norberto, Mones, Eleonora, Claire Cantone, Marie, Cialdi, Simone, Gargano, Marco, Ludwig, Nicola, Bonizzoni, Letizia, Vedda, Anna, 2015. Ionizing radiation detection by Yb-doped silica optical fibers. *Hard X-Ray, Gamma-Ray, Neutron Detect. Phys.* XVII 08. <http://dx.doi.org/10.1117/12.2190767>.
- Mijnheer, Ben, Beddar, Sam, Izewska, Joanna, Reft, Chester, 2013. In Vivo dosimetry in external beam radiotherapy. *Med. Phys. Med. Phys.* 40 (7), 070903. <http://dx.doi.org/10.1118/1.4811216>.
- Molina, P., Santiago, M., Marcazzó, J., Spano, F., Henniger, J., Cravero, W., Caselli, E., 12 2012. Radioluminescence of red-emitting Eu-doped phosphors for fiberoptic dosimetry. *Appl. Radiat. Isotopes* 71, 12–14. <http://dx.doi.org/10.1016/j.apradiso.2012.01.005>.
- Polf, J.C., Yukihiro, E.g., Akselrod, M.s., Mckeever, S.w.s., 04 2004. Real-time luminescence from Al₂O₃ fiber dosimeters. *Radiat. Meas.* 38 (2), 227–240. <http://dx.doi.org/10.1016/j.radmeas.2003.10.005>.
- Qin, S., Chen, T., Wang, L., Tu, Y., Yue, N., Zhou, J., 2013. Angular dependence of the MOSFET dosimeter and its impact on in vivo surface dose measurement in breast cancer treatment. *Technol. Cancer Res. Treat. Technol. Cancer Res. Treat.* <http://dx.doi.org/10.7785/tcrt.2012.500382>.
- Rahman, A.k.m. Mizanur, Zubair, H.t., Begum, Mahfuza, Abdul-Rashid, H.a., Yusoff, Z., Omar, Nasr Y.m., Ung, N.m., Mat-Sharif, K.a., Bradley, D.a., 05 2016. Real-time dosimetry in radiotherapy using tailored optical fibers. *Radiat. Phys. Chem.* 122, 43–47. <http://dx.doi.org/10.1016/j.radphyschem.2016.01.019>.
- Ramírez, M., Martínez, N., Marcazzó, J., Molina, P., Feld, D., Santiago, M., 10 2016. Performance of ZnSe(Te) as fiberoptic dosimetry detector. *Appl. Radiat. Isotopes* 116, 1–7. <http://dx.doi.org/10.1016/j.apradiso.2016.07.007>.
- Rucci, Alexis, Carletti, Claudia, Cravero, Walter, Strbac, Bojan, 03 2014. Use of IAEA's phase-space files for the implementation of a clinical accelerator virtual source model. *Phys. Medica* 30 (2), 242–248. <http://dx.doi.org/10.1016/j.ejmp.2013.07.127>.
- Rucci, Alexis, Carletti, Claudia, Cravero, Walter, Strbac, Bojan, 08 2016. Use of IAEA's phase-space files for virtual source model implementation: extension to large fields. *Phys. Medica* 32 (8), 1030–1033. <http://dx.doi.org/10.1016/j.ejmp.2016.07.006>.
- Salvat, F., Fernández-Varea, J.M., Sempau, J., 2006. *PENELOPE – a Code System for Monte Carlo Simulation of Electron and Photon Transport*. Nuclear Energy Agency, Barcelona.
- Santos, Alexandre M. Caraça, Mohammadi, Mohammad, Shahraam Afshar, V., 02 2015. Energy dependency of a water-equivalent fibre-coupled beryllium oxide (BeO) dosimetry system. *Radiat. Meas.* 73, 1–6. <http://dx.doi.org/10.1016/j.radmeas.2014.12.006>.
- Teichmann, T., Sponner, J., Jakobi, Ch., Henniger, J., 2016. Real time dose rate measurements with fiber optic probes based on the RL and OSL of beryllium oxide. *Radiat. Meas.* 90 (07), 201–204. <http://dx.doi.org/10.1016/j.radmeas.2016.01.015>.
- Yorke, E., Alecu, R., Ding, L., Fontenla, D., Kalend, A., Kaurin, D., Masterson-McGarry, M., Marinello, G., Matzen, T., Saini, A., Shi, J., Simon, W., Zhu, T., Zhu, X., Rikner, G., Nilsson, G., 2005. *AAPM REPORT NO. 87: Diode In Vivo Dosimetry for Patients Receiving External Beam Radiation Therapy*. Technical report. American Association of Physicists in Medicine, ISBN 1-888340-50-9 (978-1-888340-50-9).